Influence of Misfit of Desired Damping Response in Nonlinear Ground Response Analysis

Samuel Ynieста[1], Scott J. Brandenberg[2]
[1]*Department of Civil, Geological, and Mining Engineering – Ecole Polytechnique of Montréal, Montréal, QC, Canada*
[2]*Department of Civil and Environmental Engineering – University of California Los Angeles, Los Angeles, CA, USA*

ABSTRACT

Constitutive models for 1D ground response analysis typically include a modulus reduction and damping curve as input parameters, which represent the desired behavior of the soil. Most of the models use modified Masing rules to define unload/reload behavior, based on the input damping curve; however, this kind of unloading/reloading rules typically introduce a misfit of the input damping curve, resulting in a mismatch of the desired behavior. The extent to which this mismatch affects the results of a ground response analysis was previously hard to assess because of the lack of models able to provide a perfect fit of both the damping and the modulus reduction curves.

This paper presents a comparison of nonlinear ground response analyses using different models, providing different levels of goodness of fit of the input damping curve. A perfect fit of the input curve is obtained with the authors' recently developed model. This model provides a perfect match of both input curves by using a coordinate transformation technique, and controlling the soil's response in the transformed coordinate system. The results of the nonlinear ground response analyses are then used to assess the site conditions and the ground motion characteristics for which a mismatch of the damping curve can yield a significant difference in the results of a ground response analysis.

1 INTRODUCTION

One dimensional site effects are usually considered using either nonlinear site factors that depend on the average shear wave velocity in the upper 30m (V_{S30}), or site-specific one-dimensional ground response analysis. One dimensional ground response analysis can be performed using equivalent-linear (EL) or nonlinear (NL) procedures. NL simulations are superior to EL when shear strains are greater than 0.1% (Kaklamanos et al. 2015) but require a constitutive model.

Constitutive models used for 1D ground response analysis often utilize a backbone curve that is matched, in a least-squares sense, to input modulus reduction and damping (MRD) curves (Hashash et al. 2010). In order to match the input curves, the constitutive models use two sets of equations, one for initial loading, and one for unload/reload behavior.

Initial loading is controlled by the backbone curve which is calculated from the modulus reduction curve. The most common method of modeling the backbone curve is to use a hyperbolic formulation. This formulation simply fits a hyperbola to the monotonic stress-strain curve. The formulation was first introduced by Hardin and Drnevich (1972) and later modified by Matasovic and Vucetic (1993) and Darendeli (2001). Empirical models to calculate MRD curves based on simple soil properties (e.g. Darendeli 2001), often define the modulus reduction curve as a hyperbola for consistency with the assumption of a hyperbolic stress-strain curve. However, most of these empirical relationships extrapolate the curves at large strain due to a limited database. Several solutions have been proposed to match a target shear strength. Yee et al (2013) introduced a hybrid procedure where the modulus reduction curve is modified to match a shear strength at high strains and obtain a more reasonable backbone curve. If such a curve is used, models using a hyperbola will not capture the shear strength properly (Chiu et al. (2008)). Groholski et al. (2016) presented a new quadratic/hyperbolic (GQ/H) model for backbone curve, where the shear strength is an input. Yniesta (2016) uses a cubic spline fit to match an input modulus reduction curve.

The unload/reload behavior is controlled by a set of rules based on the input damping curve. Most of the constitutive models use modified Masing rules to define unload/reload behavior; however, these rules typically introduce a misfit of the input-damping curve, resulting in a mismatch of the desired behavior (Hashash et al. 2010). The model presented in Yniesta (2016) is able to match exactly any input-damping curve by using a coordinate transformation. In the transformed coordinate system, the shape of the unloading/reloading curve is controlled so that it is consistent with the input damping curve.

Previous research has assessed the influence of a misfit of a modulus reduction curve (e.g. Afacan 2014), but the influence of a misfit of the damping curve has never been studied because of the lack of a model being able to perfectly match any damping curve. This paper presents a comparison of NL ground response analyses performed with Deepsoil (Hashash et al. 2016), using different constitutive models providing a perfect fit of an input modulus reduction curve, but different goodnesses of fit of an input damping curve. The model by Yniesta (2016) was implemented in Deepsoil using the new user-defined model feature of the software in order to provide a perfect fit of the damping curve. The effect of the goodness of the fit on site response is studied on three sites of varying stiffness, shaken with three different input motions, scaled to amplitudes of 0.1g, 0.4g, and 0.7g, for a total of 108 different ground response analyses. The effect of the goodness of the fit on amplification of acceleration and maximum strain is assessed.

2 INPUT MODULUS REDUCTION AND DAMPING CURVES

2.1 Input Modulus Reduction and Damping Curves

For all the simulations, one set of curves was used throughout the entire profile, regardless of the effective stress. MRD curves are known to depend on confining pressure, but the purpose of this study is to analyze the effect of a misfit of the damping curve, all other parameters kept constant.

In order to isolate the effect of a mismatch of the damping curve, all the models should provide an identical fit of the modulus reduction curve. Therefore, we set the modulus reduction curve to have a hyperbolic form to allow all the models in Deepsoil to match it perfectly. The modulus reduction curve is based on Darendeli's empirical equations with the following properties: plasticity index (PI) =35, overconsolidation ratio (OCR) =1, number of cycles (N)=10, and frequency of loading = 1 Hz. In order for all the models to provide an exact fit of the modulus reduction curve, the input modulus reduction curve is not corrected to capture a realistic target shear strength. The damping curve was obtained by using the curves from Vucetic and Dobry (1991) implemented in Deepsoil for a PI of 35. This damping curve was selected so that all the models provide a different fit of the damping curve (as presented in the next section). Input curves are presented in figure 1. In Figure 1 G is the secant shear modulus and G_{max} is the maximum shear modulus.

2.2 Curve Fitting

In order to obtain different fits of the damping curves, four different models were used. The order of goodness of fit of the damping curve is Yniesta (2016), MRDF-UIUC (Phillips and Hashash 2009), Darendeli (2001), and Masing rules (1926). Details on the formulation of the models can be found in the cited references.

It should be noted that the goodness of the fit associated with each model pertains to the set of curves selected and is not representative of the goodness of the model. For instance, if a damping curve obtained from the empirical model by Darendeli (2001) was used with the unload/reload rules from the same reference; a perfect fit would be obtained. Figure 1 presents the input modulus reduction and damping curves, along with the different fits. Note that the fit obtained from the Masing rules is not visible at large strains, in order to better visualize the other fits. For information the damping ratio obtained with Masing rules at 10% shear strain is 52.6%. All models provide an exact fit of the modulus reduction, and therefore only the input curve is presented.

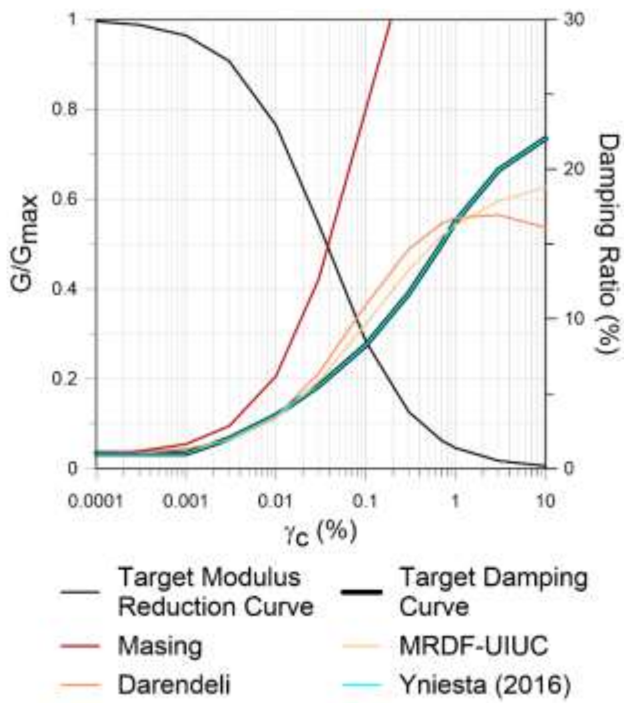

Figure 1 Input modulus reduction and damping curves

3 SITE RESPONSE ANALYSIS

Total stress nonlinear site response analyses were performed on three different profiles using Deepsoil (Hashash et al. 2016). All profiles consist of 30 meter of soil atop bedrock. The bedrock unit weight was 25 kN/m^3, its shear wave velocity was 760 m/s, and its damping ratio was 5%.

3.1 Sites Profiles

For the purpose of the study, the sites were selected to be as simple as possible, while having three different NEHRP site classes (as defined in BSSC (2001)). The unit weight of the soil was taken as 18 kN/m^3 throughout the entire profile, and the shear wave velocity was defined as increasing linearly with vertical effective stress following Equation 1, as presented in figure 2.

$$V_s = V_{s0} + V_{s1} \cdot \left(\frac{\sigma_v'}{p_a}\right) \quad [1]$$

Where p_a is the atmospheric pressure and σ'_v the vertical effective stress. V_{s0} and V_{s1} are variables which values for each site are presented in table 1. Table 1 also presents the average shear wave velocity of the site (V_{s30}), the site period (T_{site}) and frequency (f_{site}). The shear wave velocity profiles were selected for their simplicity. The soft, medium and stiff sites have site class E, D, and C, respectively.

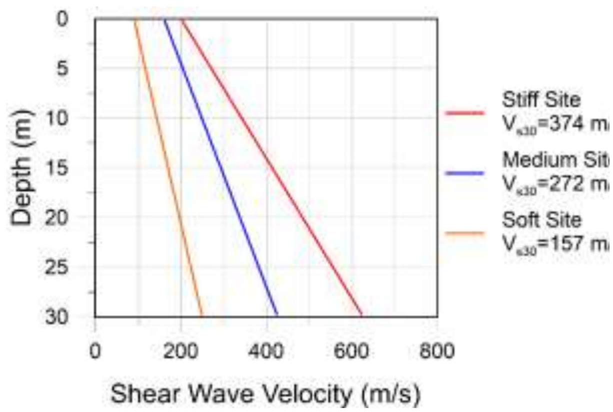

Figure 2 Shear wave velocity profiles for the three sites

Table 1 Characteristics of the sites

Site	V_{s0} (m/s)	V_{s1} (m/s)	V_{s30} (m/s)	f_{Site} (s^{-1})	T_{Site} (s)
Soft	90	30	157	1.30	0.77
Medium	160	50	272	2.27	0.44
Stiff	200	80	374	3.11	0.32

3.2 Input Ground Motions

A total of twelve batches of simulations were performed, one per profile and per goodness of fit. Nine ground motions were applied at the bottom of the soil columns for each batch of simulations. The ground motions were recordings from the Kobe, Kocaeli and Nahanni events, integrated in the version 6.1 of Deepsoil, linearly scaled in the time domain at three different PGA levels, 0.1, 0.4 and 0.7. All three time series originate from the defunct PEER strong ground motion database and were recorded on stiff ground conditions (A or B) within a relatively short distance to the fault rupture, between 0.6 and 17 km. The properties of the input ground motions are presented in table 2. Input ground motions are now available on the NGA-West2 database (Ancheta et al. 2013). In the subsequent sections the ground motions are called Kobe, Kocaeli and Nahanni for simplicity.

Figures 3a, b and c show the time series for each ground motion scaled at 0.4g. The three different ground motions were selected because they all have a peak response spectrum and peak Fourier amplitude at different periods (Figure 3d). The periods of maximum Fourier amplitude for Kobe, Kocaeli and Nahanni are 1.38s, 0.33s, and 0.12 respectively.

3.3 Results

3.3.1 Influence of a Misfit of the Input Damping Curve

This paper focuses on the effect of goodness of the fit on amplification factor and maximum mobilized shear strain. The amplification factor is defined as the surface peak acceleration divided by the PGA of the input motion. The maximum shear strain is taken as the maximum positive or negative mobilized shear strain at any depth in the profile. Amplification factors for all simulations are plotted in Figure 4 against maximum input spectral acceleration normalized by V_{s30} and site period (T_{Site}). Figure 4 shows a strong correlation between amplification factor and the normalized spectral acceleration, which proved to be the best predictor of the amplification factor.

Table 2 Input Ground Motion Properties

Motion / Properties	Kobe	Kocaeli	Nahanni
Record Number (Former PEER database)	P1043	P1087	P0498
Station's name	KJMA	Arcelik	Site 3
Component	000	000	270
Date	1995/01/16	1999/08/17	1985/12/23
Moment Magnitude	6.9	7.4	6.8
Distance to Fault Rupture (km)	0.6	17.0	16.0
USGS Site Class	B	B	A
Peak Ground Acceleration (PGA) (g)	0.821	0.218	0.148
Period of Maximum Fourier Amplitude (s)	1.38	0.33	0.12

The maximum mobilized shear strain was found to correlate strongly with input peak ground velocity (PGV_{input}) normalized by V_{s30} (Figure 5). As the ratio PGV_{input}/V_{s30} increases, whether by increasing the demand (PGV_{input}), or decreasing the resistance (V_{s30}), the maximum mobilized shear strain increases as well.

In order to compare the effect of goodness of fit we study the deviation of the predictions of all the models from the predictions of Yniesta (2016). The results are plotted in Figure 6 and 7, where the percent difference for a particular simulation is calculated as the difference between the predicted value and the value predicted by Yniesta (2016), divided by the latter. The percent difference is calculated with respect to the predictions of Yniesta (2016) because the latter provides a perfect fit of the damping curve, and therefore this percent difference represents the effect of the misfit of the damping curve. Figure 6 shows a clear correlation between the percent difference on the maximum mobilized shear strain and normalized input PGV. The maximum mobilized shear strain is under predicted at lower PGV_{input}/V_{s30} ratios by all the models, but over predicted at large ratios, except by the Masing rules model which under-predicts the mobilized shear strain for all normalized PGV. Since the target damping curve is overestimated at small strains and underestimated at large

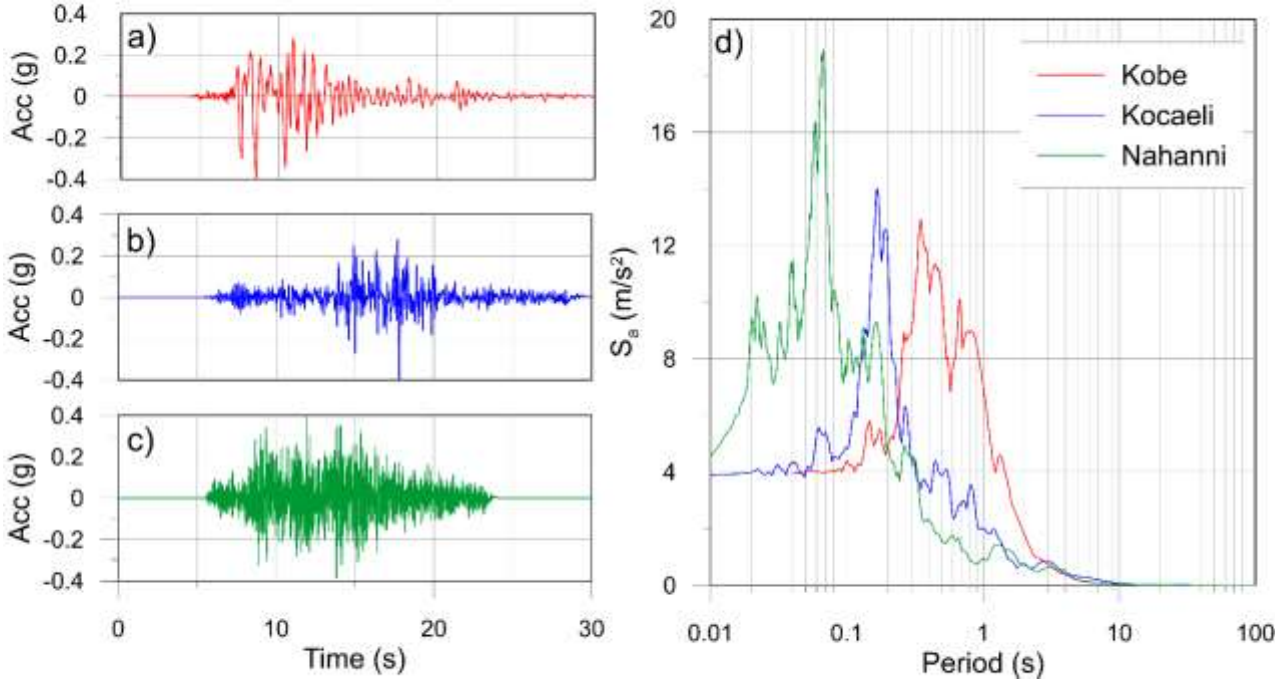

Figure 3 Input ground motions: time series (a, b, and c), and response spectra (d) scaled at 0.4g

strains by the fit induced by the MRDF-UIUC and Darendeli's model, this trend is consistent with the expected behavior. For the MRDF-UIUC model, the difference ranges from 1% at small strains, to 33% at large strains. For Darendeli's model, the difference in maximum shear strain reaches a maximum of 37%. These differences are significant, even though the fits are relatively close to the target curve. The fit resulting from the use of the original Masing Rules is overestimating the damping at all strains and therefore the strains are constantly under predicted by as much as 80%.

The percent difference on the amplification factor shows little correlation with normalized maximum spectral acceleration (Figure 7) and no trend with *PGV/V_{S30}* and *PGA.* For *PGA* and *PGV/V_{S30}* the results are not presented for the sake of brevity. However, figure 7 seems to indicate that the percent difference increases when the normalized spectral acceleration increases. The differences in amplification factor are slightly smaller than the differences in shear strain. The maximum differences are 30% and 29% for the MRDF-UIUC and the Darendeli models, respectively. Unlike for the maximum mobilized shear strain, the maximum percent difference on the amplification factor is greater for MRDF-UIUC than Darendeli. However, this represents an exception, and the general trend is that the percent difference is smaller for the MRDF-UIUC model than Darendeli's. However, this exception attests of the complexity of 1D nonlinear site response, and the difficulty of characterizing the governing parameters. Even in the simple and limited set of site response simulations presented herein, multiple parameters interact, and trends are difficult to identify.

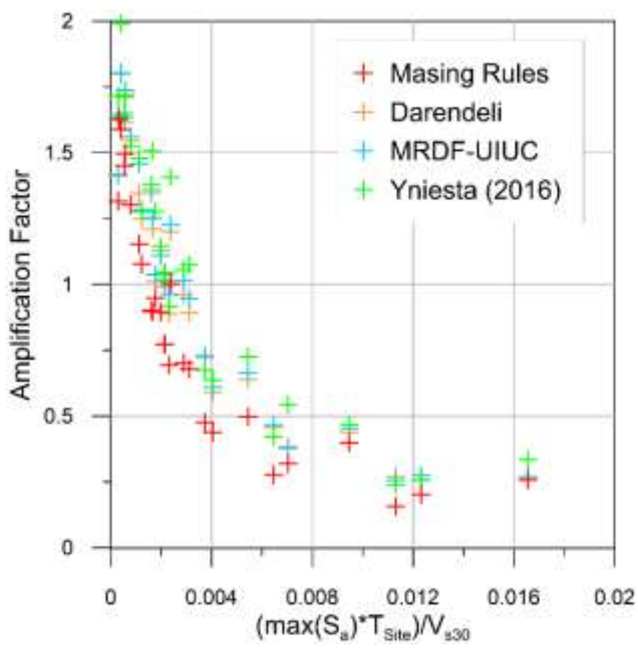

Figure 4 Amplification factor vs. normalized maximum spectral acceleration

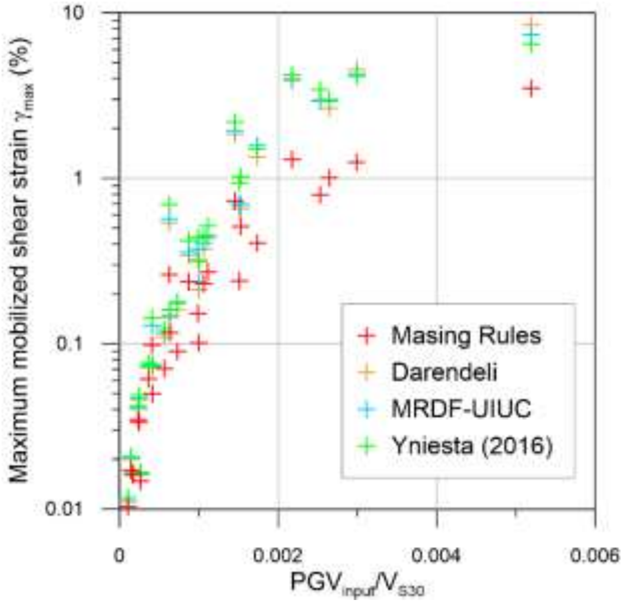

Figure 4 Maximum shear strain (γ) vs. normalized PGV

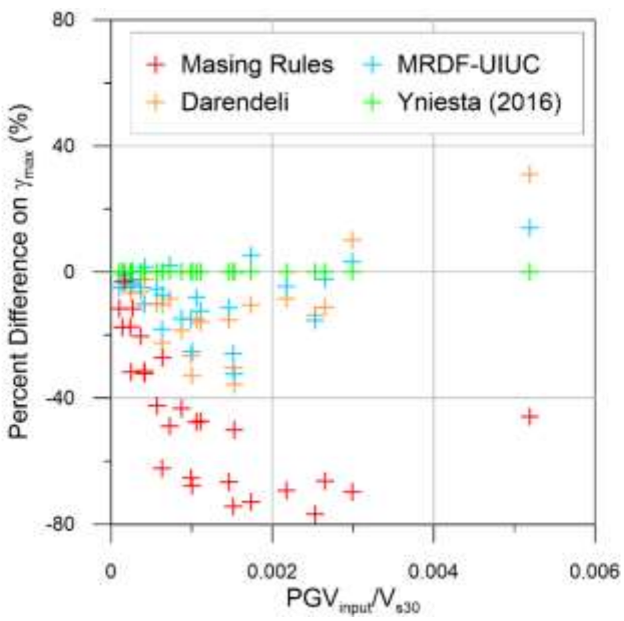

Figure 5 Difference on γ vs. normalized PGV

3.3.2 Comparison of Response Spectra and Maximum Mobilized Shear Strain

In order to compare the predictions of the different models, response spectra of surface motions and profiles of maximum mobilized shear strain are plotted for each model. Figures 8a and 8c compare the predictions for the Kocaeli motion scaled at 0.1g on the site with medium stiffness. At this PGA level, strains are low, and the predictions of all models do not differ vastly, except for that of the Masing rules model. The relatively small difference in the predictions is explained by the *PGV/V_{S30}* ratio, which

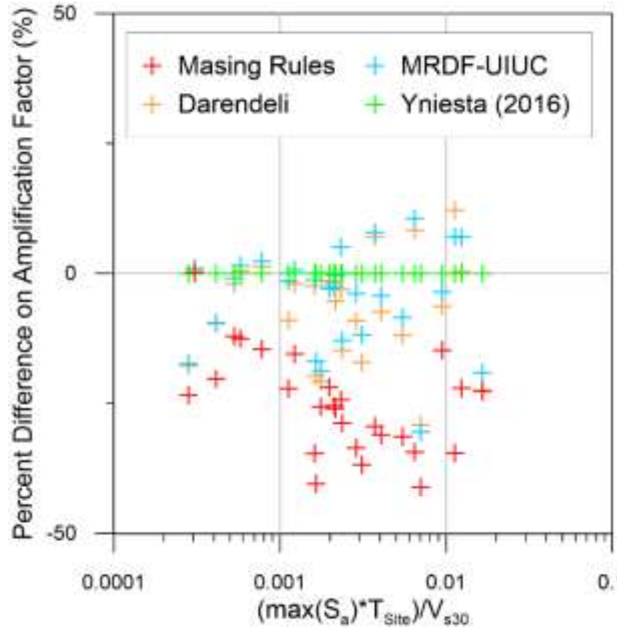

Figure 7 Difference on amplification factor vs. normalized maximum Spectral Acceleration

in this case is only 0.00024, thus inducing low strains (about 0.04%).

On the other hand, figures 8b and 8d compare the predictions for the case of a soft site shaken with the Kocaeli motion scaled at 0.4g. At this PGA level the *PGV/V_{S30}* ratio is 0.0015, or about six times larger than in the previous example. This ratio induces larger shear strains (from 0.24 to 0.95%, depending on the model), at which the models are over-predicting the damping, resulting in an underestimation of the mobilized shear strain and surface PGA.

These site conditions and specific motions were selected for these examples because the four models predict a similar depth of maximum mobilized shear strain, which is not always the case in the other simulations.

4 CONCLUSIONS

This paper presented a comparison of total stress nonlinear site response analyses performed in Deepsoil with four different constitutive models. The input parameters were chosen so that the four models would provide a perfect fit of the input modulus reduction curve, but different goodnesses of fit of the damping curve. The effect of the goodness of the fit of the damping curve on site response was evaluated by analyzing ground response of three different sites of different stiffnesses, shaken by nine different ground motions of different amplitudes and different dominant periods. The effect of the goodness of the fit on amplification factors and maximum shear strain was studied and the following conclusions were reached:

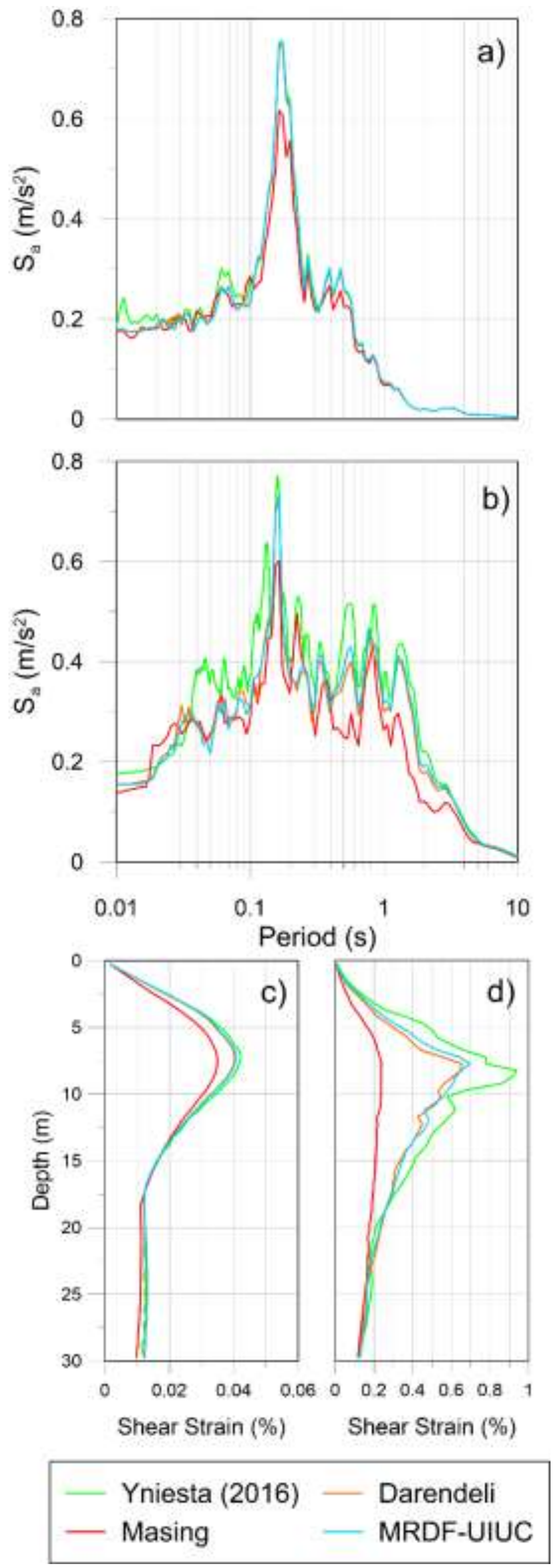

Figure 8 Response spectra and mobilized maximum shear strain profiles for Kocaeli scaled at 0.1g on a site of medium stiffness (a and c) and Kocaeli scaled at 0.4 g on a soft site (b and d)

- A modest misfit of the damping curve can lead to a large difference in the calculation of maximum mobilized shear strain;
- The amplitude of the difference in maximum shear strain depends on the ratio PGV/V_{s30}, and on which portion of the damping curve is misfit;
- The difference on amplification factor is lower than the difference in shear strain but can still be significant. The difference showed no correlation with the predictive variables studied herein;

Note that the present study focuses on the effect of the misfit of the damping curve. However, the behavior of a soil model for 1D site response analysis is not characterized solely by its ability to match the input curves, but also by its behavior during small unload/reload cycles. For example, two models with fundamentally different unload/reload rules might provide the same fit of a given damping curve, but the behavior during small unload/reload cycle within large amplitude cycles might be different, which will impact the site response. The extent to which the formulation of a constitutive model will influence site response is difficult to quantify with the present set of simulations and is beyond the scope of this study.

5 ACKNOWLEDGMENTS

The authors would like to thank Benjamin Turner from Dan Brown and Associates, for the help he provided with the post-processing of Deepsoil results. The authors would also like to thank Professor Yousef Hashash and Michael Musgrove for helping with the implementation of the authors' model in Deepsoil.

6 REFERENCES

Afacan, K. B. 2014. Evaluation of Nonlinear Site Response of Soft Clay Using Centrifuge Models. Ph.D. Dissertation, University of California, Los Angeles, CA, USA.

Ancheta, T. D., Darragh, R. B., Stewart, J. P., Seyhan, E., Silva,W. J., Chiou, B. S.-J., Wooddell, K. E., Graves, R. W., Kottke, A. R., Boore, D. M., Kishida, T., and Donahue, J. L., 2013. *PEER NGA-West2 Database*, PEER Report No. 2013/03, Pacific Earthquake Engineering Research Center, University of California, Berkeley, CA, 134 pp.

Chiu, P., Pradel, D.E., Kwok, A.O.L. and Stewart, J.P. 2008. Seismic response analyses for the Silicon Valley Rapid Transit Project, *Proc. 4th Decennial Geotechnical Earthquake Engineering and Soil Dynamics Conference*, ASCE, Sacramento, CA

Darendeli, M. 2001. Development of a new family of normalized modulus reduction and material damping curves. Ph.D. Thesis, Dept. of Civil Eng., Univ. of Texas, Austin.

Groholski, D. R., Hashash, Y. M., Kim, B., Musgrove, M., Harmon, J., & Stewart, J. P. 2016. Simplified Model for Small-Strain Nonlinearity and Strength in 1D Seismic Site Response Analysis. *Journal of Geotechnical and Geoenvironmental Engineering*, ASCE 04016042.

Hardin, B.O. and Drnevich, V.P. 1972. Shear modulus and damping in soils: design equations and curves, *Journal of the Soil Mechanics and Foundations Div.*, ASCE, 98 (SM7), 667–692

Hashash, Y. M. A., Phillips, C., and Groholski, D. R. 2010. Recent advances in non-linear site response analysis., *Fifth International Conference on Recent Advances in Geotechnical Earthquake Engineering and Soil Dynamics,* San Diego 2010.

Hashash, Y.M.A., Musgrove, M.I., Harmon, J.A., Groholski, D.R., Phillips, C.A., and Park, D. 2016. DEEPSOIL 6.1, User Manual. Urbana, IL, Board of Trustees of UI at Urbana-Champaign

Kaklamanos, J., Baise, L. G., Thompson, E. M., & Dorfmann, L. 2015. Comparison of 1D linear, equivalent-linear, and nonlinear site response models at six KiK-net validation sites. *Soil Dynamics and Earthquake Engineering*, 69, 207-219.

Matasovic, N. and Vucetic M. 1993. Cyclic Characterization of Liquefiable Sands, *Journal of Geotechnical Engineering*, ASCE, 119(11), 1805-1822

Masing, G. 1926. Eigenspannungen and verfertigung beim messing. *Proc. 2nd International Congress on Applied Mechanics*, Zurich, Switzerland

Building Seismic Safety Council (BSSC) 2001. NEHRP recommended provisions for seismic regulations for new buildings and other structures, 2000 Edition, Part 1: Provisions, prepared by the Building Seismic Safety Council for the Federal Emergency Management Agency (Report FEMA 368), Washington, D.C

Phillips, C., and Hashash, Y. M. A. 2009. Damping formulation for nonlinear 1D site response analyses, *Soil Dynamics and Earthquake Engineering*, 29(7), 1143-1158.

Vucetic, M., & Dobry, R. 1991. Effect of soil plasticity on cyclic response, .*Journal of Geotechnical Engineering*, ASCE, 117(1), 89-107.

Yee E., Stewart, J.P., Tokimatsu, K. 2013. Elastic and large-strain nonlinear seismic site response from analysis of vertical array recordings, *Journal of Geotechnical and Geoenvironmental Engineering, ASCE* 139 (10), 1789-1801.

Yniesta, S., 2016. Constitutive Modeling of Peat in Dynamic Simulations. Ph.D. Dissertation, University of California, Los Angeles, CA, USA.